FATIGUE STRENGTH IN PRESENCE OF SHALLOW DEFECTS UNDER TORSION

Stefano Beretta, Khaydar Valiullin

Department of Mechanical Engineering, Politecnico di Milano, via La Masa 34 – 20156 Milano, e-mail: stefano.beretta@polimi.it

ABSTRACT
Fatigue strength in presence of inhomogeneities is controlled by the threshold condition of small cracks which nucleate at the defect tip. In biaxial in-phase fatigue strength is controlled by the threshold condition of small cracks at Mode I branches. This paper presents the results of set of torsional fatigue tests in presence of shallow micronotches for a gear steel. The results show that the fatigue strength mechanism under torsion is controlled by the competition between Mode I and Mode III propagation.

1. INTRODUCTION

Fatigue strength in the presence of inhomogeneities is controlled by the threshold condition of small cracks which nucleate at the defect tip. Therefore, the fatigue limit is associated with the threshold condition of small cracks [1]. In the case of torsional fatigue it has been shown that for round defects the fatigue strength under bi-axial loading is controlled by the presence of mode I small cracks, whose threshold condition is a function of stress bi-axiality [2]. In accordance with this concept, fatigue limit under torsional loading, in presence of surface spherical defects, is approx. 85% of the fatigue limit under tension as it has been found by Endo [3] for cast iron. It therefore follows that if the threshold condition of small cracks under torsion is characterized by the formation of Mode I branches, fatigue strength can then be predicted by knowing the relationship between Mode I ΔK_{th} and crack size (as it was shown by Murakami Takahashi [4]). However, som e mechanical components subected to torsion (e.g. automotive half-shafts) show fatigue failures characterised by shear crack propagation triggered by shallow longitudinal defects.

This paper presents the results of different sets of torsion fatigue tests which use shallow micronotches on a high strength gear steel. The results show that crack advance mechanism is controlled by the competition between Mode I and Mode III propagation even when the failure mode is to be one of the two failure modes (usually Mode I).

2. TORSIONAL FATIGUE OF SHALLOW MICRO-NOTCHES

2.1 Gear steel

The first series of torsional fatigue experiments were carried out onto a gear steel (UTS= 2100 MPa, yield strength = 1480 MPa; cyclic 0.2% proof stress = 850 MPa) Cyclic curve has been interpolated by Ramberg-Osgood equation with parameters H = 1598.9 MPa, n = 0.100925. it can be noticed strong strain softening of the material.

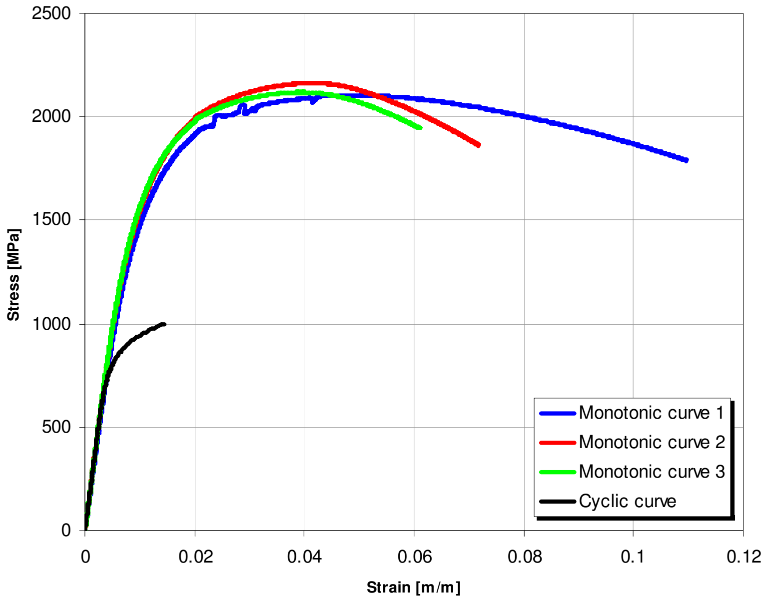

Fig.1 - Monotonic and cyclic curves

2.1.1 Bending fatigue tests

Specimens which had been subected to a series of b ending fatigue tests (R=-1) with micronotched specimens (∅=8 mm) in order to accurately determine the relationship between bending fatigue strength and crack size. The defects adopted for bending Fatigue tests have been obtained by EDM machining (see Fig. 2) after a careful electro polishing of specimens. Fatigue limit test have been carried on a resonance bending/torsional machine by means of short “stair case” sequence (test interrupted after $12 \cdot 10^6$ cycles).

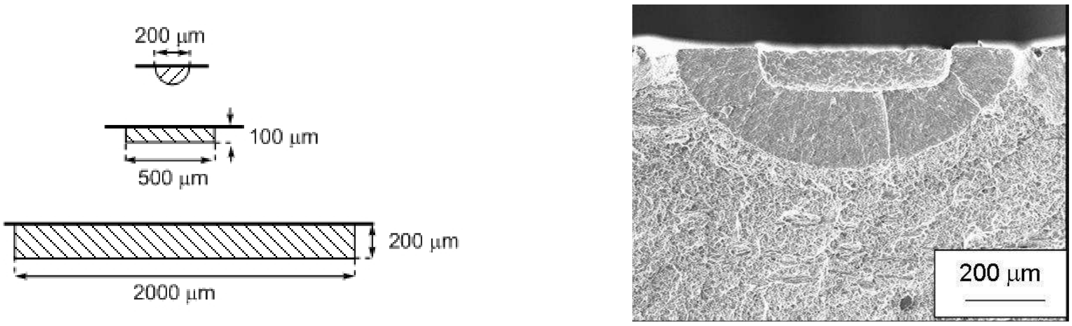

(a) (b)

Fig.2 – Bending fatigue tests: a) micronotches geometry, b) Fracture surface of 100x500 μm defect

Fatigue test results have been interpolated with a modified version of El-Haddad model (see Fig.3.a) [5]:

$$\Delta\sigma_w = \Delta\sigma_{wo} \cdot \sqrt{\frac{\sqrt{area_o}}{\sqrt{area} + \sqrt{area_o}}} \tag{1}$$

Since specimens survived to fatigue tests showed the presence of non-propagating cracks (see Fig.4), fatigue limit corresponds to the threshold condition of this cracks. In particular it was possible to estimate ΔK with equation [6]:

$$\Delta K = 0.65 \cdot \Delta S \cdot \sqrt{\pi \cdot \sqrt{area}} \tag{2}$$

Correspondingly fatigue limit test results were transformed into threshold data, described by the equation (see Fig. 3.b):

$$\Delta K_{th} = \Delta K_{th,LC} \cdot \sqrt{\frac{\sqrt{area}}{\sqrt{area} + \sqrt{area_o}}} \tag{3}$$

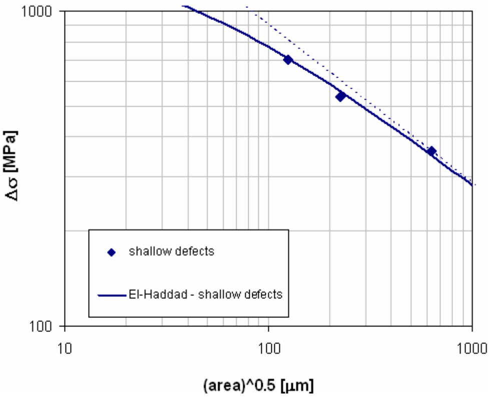

(a)

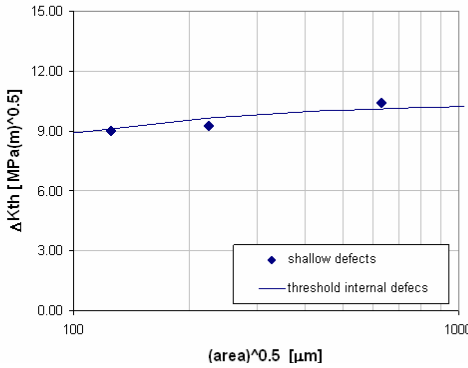

(b)

Fig.3 – Fatigue strength under bending: a)Kitagawa showing data interpolation with the modified El-Haddad model, b) threshold model variation of the ΔK_{TH} with crack size

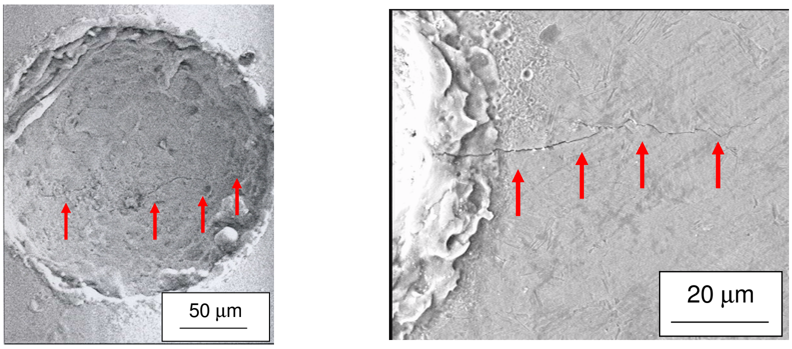

Fig.4 - Non-propagating cracks at the tip (or bottom) of the defects

2.1.2 Torsional tests

Similar experiments were carried out under torsion with longitudinal shallow notches (EDM machined after electro polishing specimens' surface) with sizes of 100×500 m (depth × length) and 100 ×1000 m.

(a)

(b)

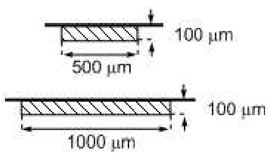

(c)

Fig.5 – Torsional fatigue tests on gear steel: a) equipment for torsional test; b) specimen; c) micronotches adopted in torsion tests.

Table 1 – Torsional tests on gear steel

defect type	√area m	$\Delta\tau_w$ MPa	τ_w/σ_w	predicted τ_w MPa
100×500	225	660	1.19	686
100×1000	330	565	1.20	553

Results of the fatigue limit tests in alternating torsion (tests were carried out with stair-case sequences and they were interrupted after $12{\cdot}10^6$ cycles) are shown in Tab. 1. It is interesting to note that the ratio τ_w/σ_w is completely different from the typical value for round defects [4,7]. Observing run-outs specimens it is possible to see that below τ_w there is the formation of longitudinal non-propagating Mode III shear cracks at the bottom of the notch (in the central part) which form branches at 45° (towards the end of the defect). Failures occur on fracture planes at 45% which coincide with the non-propagating branches. (see Fig.7)

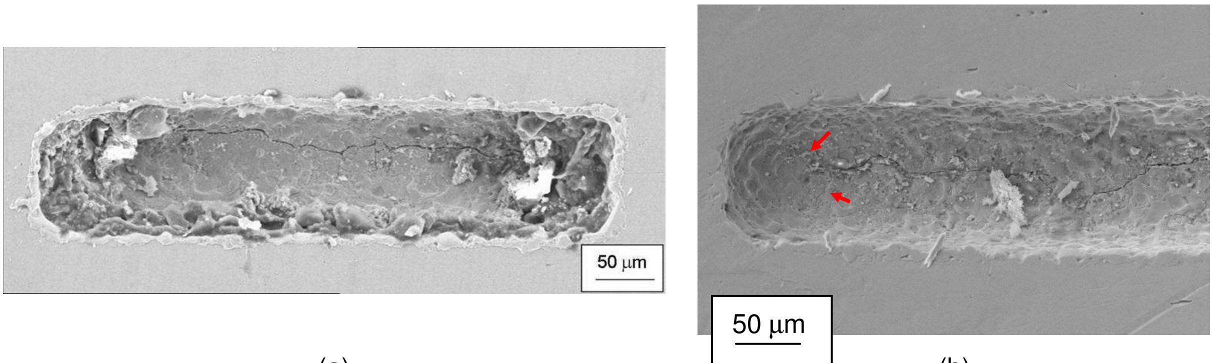

(a) (b)

Fig.6 - Run-out specimens : a)100x500 µm defect; b) 100x1000 µm with Mode I branching

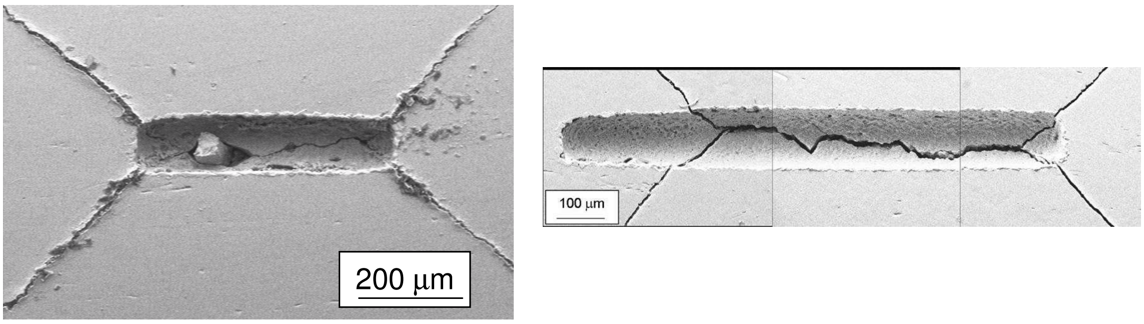

(a) (b)

Fig.7 – Fractographies of torsional tests on gear steel: a) broken specimen with a 100×500 m defect; b) non propagating shear cracks at the bottom of the notch for run-out specimen with a 100×1000 m defect.

3. ANALYSIS OF FATIGUE STRENGTH

Analyzing the fracture mechanism, it can be said that the torsional fatigue limit coincides with the threshold condition for propagation of Mode I branches. When a crack is loaded in Mode III, according to Pook [8], propagation should occur onto tilted facets at θ=45° which maximizes K_I so that:

$$K_{I,\vartheta=45^\circ} = K_{III} \tag{4}$$

In fact, by calculating Mode III SIF for shear longitudinal cracks at the tip of micro-notches with geometric factors by Kassir Sih [9], which give a good approximation for semi-elliptical surface flaws [10], it was possible to observe that torsional fatigue strength corresponds to $\Delta K_{th,I}$ for small cracks on prospective facets at 45°. On the other hand, by adopting the same method it was possible to obtain very good predictions of τ_w (see Tab. 1).

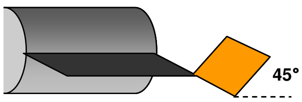

(a)

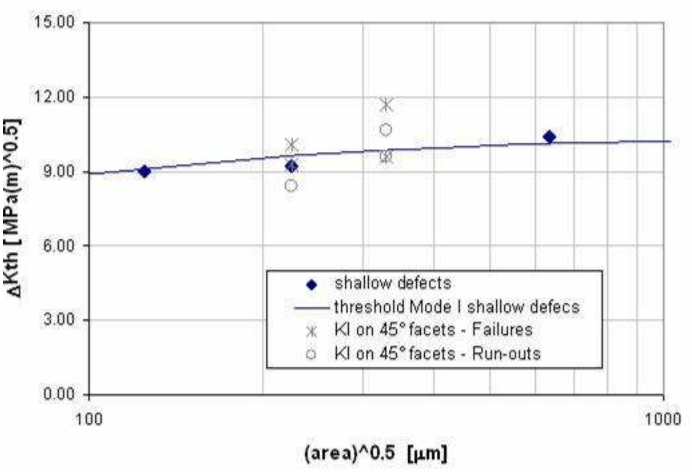

(b)

Fig.8 – Estimation of the fatigue strength under torsion: a) threshold mechanism for fatigue stresngth under torsion, b) threshold results

Two points are worth remarking: i) the crack size in this analysis of small cracks' is expressed by √area parameter by Murakami [6] and not by crack depth; ii) threshold is controlled by Mode III-Mode I facets at the bottom of the notch since Mode III is predominant because of the micro-notch shape (while for semi-circular cracks threshold is controlled by Mode II-Mode I branching at surface tips [4]). Moreover results tend to show a dependence on defect size similar to the on of Mode I [11]

4. CONCLUDING REMARKS

In this paper some experimental results about torsional fatigue strength in presence of shallow micro-notches have been presented showing that: i) fatigue strength of micronotches is controlled by the development of Mode I branches at the tip of shear cracks; ii) pre-cracked micronotches can induce stable Mode III propagation. This stable propagation was also evidenced by shear Mode III propagation ahead of the micronotch as evidenced by polished sections (see Fig. 9).

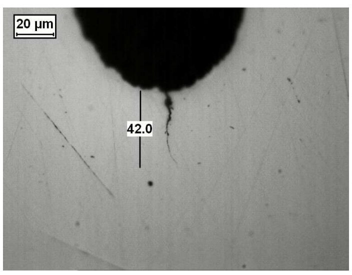

(a)

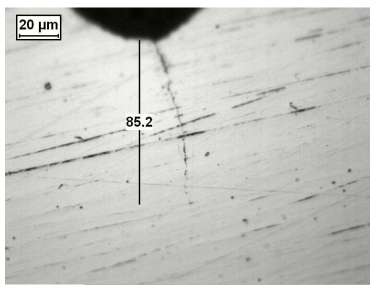

(b)

Fig.9 - Transverse sectioning of a run-out specimen defect size 100x1000 μm, a) image taken at about 140 μm from one side of the crack, b) image taken at about 290 μm

REFERENCE LIST

[1] Murakami, and Endo, M., *Int. J. Fatigue*, **Vol. 16**, 1994, pp. 163-181.

[2] Beretta, S. and Murakami, ., *Fat. Fract. Engng. Mater. Struct.*, **Vol. 23**, 2000, pp. 97-104.

[3] Endo, M., *Trans. J. Soc. Mat. Sci.* , **Vol. 45**, 1996, pp. 16-20.

[4] Murakami, . and Takahashi, K., *Fat. Fract. Engng. Mater. Struct.*, **Vol. 21**, 1998, pp. 1473-1484.

[5] Beretta, S., Propagation of short cracks in a high strength steel for railway axles, in *Proc. ECF14 Conference*, Cracow, 2002.

[6] Murakami, ., *Eng. Fract. Mech.*, **Vol. 22**, 1985, pp. 101-114.

[7] Murakami, ., Takahashi, K., Kusumoto, R., *Fat. Fract. Engng. Mater. Struct.*, **Vol. 26**, 2003, pp. 523-531.

[8] Pook, L.P., *Crack Paths*, WitPress, Southampton, UK, 2002 .

[9] Kassir MK, Sih GC, E. *J. Appl. Mech*, Trans. ASME, **Vol 33**, 1966, pp. 601-611.

[10] He, M. . Hutchinson, J.W., *Eng. Fract. Mech.*, **Vol. 65**, 2000, pp. 1-14.

[11] Toyama K., Takahashi K., Murakami ., Crack gr owth mechanism and crack size dependency of Mode II and Mode III fatigue crack threshold. JSME-MMD. 2003.